ELSEVIER

Polymer 42 (2001) 8959–8964

polymer

www.elsevier.com/locate/polymer

Surface relaxation behavior of proton- and perfluoroalkyl-terminated poly(2-vinylpyridine) films

Xiqun Jiang[a,b], Keiji Tanaka[a], Atsushi Sakai[a], Atsushi Takahara[c], Tisato Kajiyama[a,*]

[a]*Department of Applied Chemistry, Faculty of Engineering, Kyushu University, Fukuoka 812-8581, Japan*
[b]*College of Chemistry and Chemical Engineering, Nanjing University, Nanjing 210093, People's Republic of China*
[c]*Institute for Fundamental Research of Organic Chemistry, Kyushu University, Fukuoka 812-8581, Japan*

Received 26 February 2001; received in revised form 24 April 2001; accepted 24 April 2001

Abstract

Proton- and perfluoroalkyl-terminated poly(2-vinylpyridine) (P2VP–H and P2VP–$C_2C_8^F$) were anionically synthesized. Surface molecular motions of P2VP–H and P2VP–$C_2C_8^F$ films prepared on hydrophilic silicon wafers were examined by lateral force microscopy (LFM). Surface glass transition temperature, T_g^s, of P2VP–$C_2C_8^F$ was lower than that of P2VP–H probably due to the difference of the surface concentration of chain ends. Also, both T_g^s values were lower than each corresponding bulk glass transition temperature, T_g^b. Surface molecular motion in an ultrathin film was less activated than that of the thick film, although T_g^s in the ultrathin film remained lower than T_g^b. In the case of ultrathin films, the surface/interface area to volume ratio becomes larger, and thus the thermal molecular motion at the surface is affected by that at the polymer/substrate interface. Since molecular mobility on the substrate might be restricted owing to the polar attractive interaction between polymer segments and the hydrophilic substrate, the activation of surface molecular motion apparently turns weak for such an ultrathin film. © 2001 Elsevier Science Ltd. All rights reserved.

Keywords: Poly(2-vinylpyridine); Surface glass transition; Lateral force microscopy

1. Introduction

Surface structure and properties of polymers, which are fairly different from those in bulk, are of importance for scientific interests and technological applications such as coatings, adhesives tribomaterials, biomaterials, etc. [1,2]. In addition, since these materials have been generally used as thin films, aggregation states and physical properties of thin films should be systematically elucidated.

So far many groups have worked on glass transition behavior of thin films, and a notion has already emerged that glass transition behavior of thin films is much different from that of bulk ones [3–8]. However, a contradictory dependence of glass transition temperature, T_g, on the film thickness has been reported. In the case of supported and freely-standing polystyrene (PS) films, T_g decreased with decreasing thickness. On the other hand, in the case of poly(methyl methacrylate) (PMMA) [9,10] or poly(2-vinylpyridine) (P2VP) [11] on hydrophilic substrate, it was found that T_g of the thin film increased with a decrease in the thickness. The film thickness dependence of T_g for PMMA or P2VP on the hydrophilic substrate was explained in terms of the existence of an immobile layer on the substrate, resulting from an attractive interaction between polymer chains and substrate. These results imply that interfacial effects on T_g of thin and ultrathin films, which is defined as a film thinner than the unperturbed chain dimension, can no longer be trivial on account of a large interfacial area to volume ratio. Hence, to rationalize T_g of thin films, it is pivotal important to understand how T_g at interfaces including surface is different from that in the bulk, if any.

We have successfully applied a family of scanning force, lateral force and scanning viscoelasticity microscopes [12] (LFM and SVM), to study surface rheological properties of monodisperse PS thick films with various molecular weights [13–16] and chain end groups [17–19] on silicon wafers, and revealed that T_g at the surface, T_g^s, was much lower than the corresponding bulk T_g, T_g^b. The active molecular motion observed at the surface could be mainly interpreted by the surface segregation of chain ends and the existence of free space on the surface [16]. However, we have not known whether glass transition behavior at the surface in thin and ultrathin films is the same as that in the thick one.

---

[*] Corresponding author. Address: Department of Applied Chemistry, Faculty of Engineering, Kyushu University, Fukuoka 812-8581, Japan. Tel.: +81-92-642-3558; fax: +81-92-651-5606.

E-mail address: kajiyama@cstf.kyushu-u.ac.jp (T. Kajiyama).

PII: S0032-3861(01)00384-6

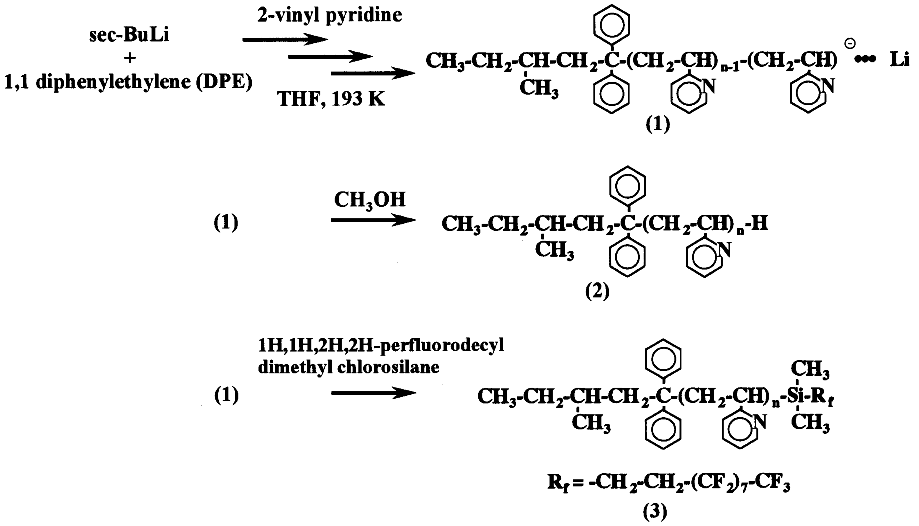

Fig. 1. Synthetic route of P2VP–H and P2VP–$C_2C_8^F$.

The objective of this paper is to investigate surface relaxation behavior of P2VP thin and ultrathin films with two kinds of chain ends prepared on hydrophilic silicon wafers. Since P2VP has strong attractive interaction with hydrophilic substrate [11], it is of interest to study how surface relaxation behavior of the P2VP thin and ultrathin films prepared on the hydrophilic substrates is influenced by a P2VP/substrate interfacial interaction. The film thickness dependence of T_g^s for PS thin and ultrathin films will be reported elsewhere [20].

2. Experimental

2.1. Materials and polymerization

2-Vinylpyridine (2VP) was dried over CaH_2 for 24 h and distilled twice under vacuum. The purified monomer was stored under argon atmosphere. The monomer was treated with triethylaluminium just prior to use, and then, vacuum-distilled again. 1,1-Diphenylethylene (DPE) was vacuum-distilled over CaH_2 and *n*-butyllithium. Tetrahydrofuran (THF) was distilled after refluxing for 24 h over sodium and benzophenone under nitrogen atmosphere. *sec*-Butyllithium (*sec*-BuLi) and 1H, 1H, 2H, 2H-perfluorodecyl dimethyl chlorosilane were used just as received.

Poly(2-vinylpyridine) terminated with proton (P2VP–H) and fluoroalkylsilane end group (P2VP–$C_2C_8^F$) were prepared by a sequential anionic polymerization using *sec*-butyllithium as an initiator in THF under argon atmosphere at 195 K. Fig. 1 shows the synthetic route of P2VP–H and P2VP–$C_2C_8^F$. At first, THF was transferred into a glass reactor by a capillary technique. Then, the reactor was cooled at 195 K, and the calculated amount of mixture of *sec*-butyllithium and DPE was added to a well-stirred THF solution by a syringe. Next, the desired amount of 2-vinylpyridine monomer was added. After 60 min at 195 K, the 3–5 fold excess amount of methanol or 1H, 1H, 2H, 2H-perfluorodecyl dimethyl chlorosilane was added to the reactor to prepare proton- and fluoroalkylsilane-terminated P2VP polymers, respectively. The polymers were precipitated in hexane and vacuum-dried. Finally, the fluoroalkylsilane-terminated P2VP were dissolved by THF and re-precipitated twice in daiflon S-3 (1,1,2-trichloro-1,2,2-trifluoroethane) in order to remove any unreacted fluoroalkylsilane terminating agents.

Table 1
Characterizations of P2VP used in this study

End groups	M_n	M_w/M_n	T_g^b (K)
–H	33k	1.16	373
–$C_2C_8^F$	33k	1.16	374

2.2. Characterization of polymers

The number-average molecular weight, M_n, and the molecular weight distribution, M_w/M_n, of the polymers obtained, where M_w denotes the weight-average molecular weight, were determined by gel permeation chromatography (GPC) (L-6000, HITACHI Co., Ltd) with polystyrene standard. Dimethylformamide (DMF) was used as an eluent for GPC measurement. In order to evaluate T_g^b of the polymers, differential scanning calorimetry (DSC) (Rigaku thermoflex 8230) measurement was carried out. The specimen was heated up to 443 K at a heating rate of 10 K min^{-1} under nitrogen purge. Table 1 shows M_n, M_w/M_n and T_g^b of the synthesized polymers. The functionality of the fluoroalkylsilane end groups was evaluated to be more than 0.8 by nuclear magnetic resonance spectroscopy. Hereafter, the samples are designated based on their end groups. That is, P2VP–H and P2VP–$C_2C_8^F$ represent the P2VP terminated by proton and fluoroalkyl end group, respectively.

2.3. Film preparation

P2VP thin films were prepared by a spin-coating method from a DMF solution onto silicon wafers at room temperature. The film thickness was controlled by the spinning rate and/or the solution concentration. In order to enforce the interaction between polymer and substrate, silicon wafer was treated as hydrophilic. Si (111) wafer was placed in a mixture solution of concentrated H_2SO_4 and 30% H_2O_2 (70/30 v/v) at 363 K for 3 h, and then washed by deionized water for several times. The prepared polymer films were dried under vacuum at room temperature for 72 h and then, at 423 K for 48 h. The film thickness before annealing was measured by using ellipsometer (M-150, JASCO Co., Ltd).

2.4. Surface characterization

The surface concentration of chain end groups was evaluated by XPS (ESCA-850, Shimadzu Co., Ltd) with MgKα at 8 kV and 30 mA. The chamber of XPS was maintained at 10^{-6} Pa. The analytical depths, $d = 3\lambda \sin\theta$, were calculated by using the value of inelastic mean-free path, λ, of photoelectrons based on Ashley's equation [21]. The magnitudes of d were 4.8, 6.8 and 9.7 nm at the emission angles of photoelectrons θ of 30, 45 and 90° respectively.

Surface relaxation behavior of P2VP films was studied by using LFM (SPA 300HV with SPI 3800 controller, Seiko Instruments Industry Co., Ltd). LFM measurement was carried out at various temperatures under vacuum in order to avoid surface oxidation and capillary force effect. A piezoscanner was thermally insulated from the heating stage. A commercially available silicon nitride (Si_3N_4) tip on a rectangular cantilever with a bending spring constant of 0.09 N m^{-1} (Olympus Co., Ltd) was used. The normal force to the cantilever tip was set to be 10 nN in a repulsive force region. Both sides of the cantilever were coated with gold in order to reduce the temperature-induced bending of the cantilever, due to the difference in the thermal expansion coefficients between Si_3N_4 and gold, as small as possible.

3. Results and discussion

First, XPS measurement was employed to examine whether chain end groups are enriched at the film surface. Fig. 2 shows the depth dependence of surface (F/C) ratio for P2VP–$C_2C_8^F$ film with a thickness of 145 nm prepared on hydrophilic silicon wafer. The sin θs of 0.50, 0.70 and 1.0 correspond to the analytical depth ranges of 0–4.8, 0–6.8 and 0–9.7 nm, respectively. The surface (F/C) ratio at all analytical depths was much higher than that in the bulk, marked by the dotted line in Fig. 2. Also, the surface (F/C) ratio significantly increased with decreasing analytical depth. Thus, it is conceivable that the fluoroalkyl chain ends are preferentially segregated at the surface. In the case of P2VP–H film, it is impossible to detect surface segregation of chain ends based on XPS. However, since the chain ends of the P2VP–H also have lower surface free energy and higher freedom than those of the main chain part, it is plausible that chain ends are concentrated at the surface of the P2VP–H film. The surface segregation of chain ends, which consisted of repeating units terminated by proton, was reported by Affrossman et al. using static secondary ion mass spectroscopy [22].

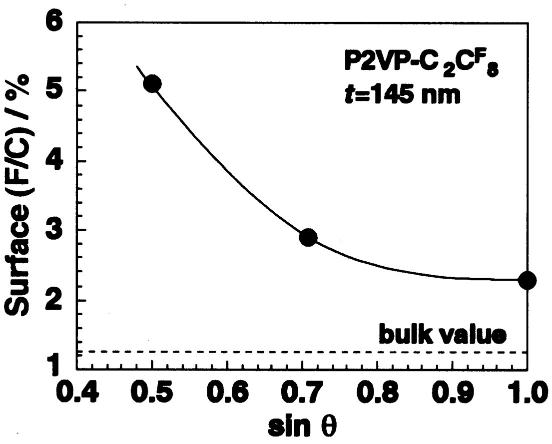

Fig. 2. Surface (F/C) variation with analytical depth for the P2VP–$C_2C_8^F$ film. Smaller value of sin θ corresponds to more surface sensitive. The dotted line corresponds to the bulk value.

Since the frictional behavior of polymeric solids is closely related to their viscoelastic properties [23], it is possible to examine the surface molecular motion of the polymeric solids using LFM [14,16,24]. Lateral force alteration with scanning rate corresponds well to the frequency dependence of dynamic loss modulus. In either case the polymer surface is completely in a glassy or rubbery state, the magnitude of lateral force is not strongly dependent on the scanning rate at a given temperature. On the contrary, the lateral force discernibly varies with the scanning rate and a peak is observable on the lateral force–scanning rate curve when the surface is in a glass–rubber transition state. Hence, if the lateral force changes with the scanning rate, it can be judged that the surface is in a glass–rubber transition state. Since the scanning rate range of our LFM is restricted within a few decades, it is impossible to obtain the whole picture of surface relaxation phenomena from a glassy to a rubbery state at a given temperature. Thus, the lateral force measurement was performed at various temperatures in order to apply a more detailed rheological analysis.

Fig. 3(a) shows the scanning rate dependence of lateral force as a function of temperature for the 140 nm thick P2VP–H film prepared on hydrophilic silicon wafer. This thickness was sufficient to avoid any ultrathinning effects on surface molecular motion. At a temperature lower than 333 K, the lateral force was invariant with respect to the

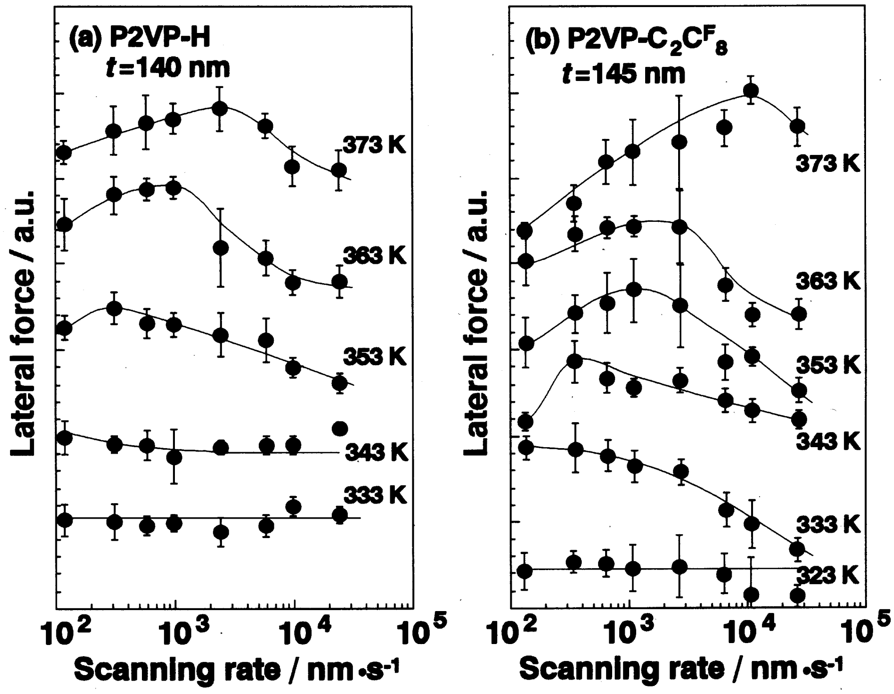

Fig. 3. Scanning rate dependence of lateral force as a function of temperature; (a) P2VP–H, (b) P2VP–$C_2C_8^F$.

scanning rate employed, implying that the surface was in a glassy state at this temperature range. On the contrary, the clear peak was observed on the lateral force–scanning rate curve at a temperature higher than 353 K, and its position shifted to a higher scanning rate with increasing temperature. These results clearly indicate the successive change of the surface molecular motion from a glassy state to the glass–rubber transition with increasing temperature. While T_g^b by DSC was evaluated to be 373 K,[1] it is apparent from Fig. 3(a) that the surface reached a glass–rubber transition state even at 353 K. That is, the surface molecular motion is more active than that in the bulk. Also, it is noteworthy that T_g of the P2VP–H thin film on the hydrophilic silicon wafer has been reported to be higher than T_g^b by virtue of the specific interaction between polymer segments and substrate [11]. This means that T_g^s in the P2VP–H thin film is totally different from T_g of the thin film itself. Since chain ends of the P2VP–H might be preferentially segregated at the surface as discussed before, an excess free volume is induced at the surface on account of the larger freedom of chain ends. Such a situation definitely makes thermal molecular motion active.

Fig. 3(b) shows the scanning rate dependence of lateral force for the P2VP–$C_2C_8^F$ film prepared on the hydrophilic silicon wafer. The film thickness was 145 nm, which was almost the same as that of the P2VP–H film, to study an effect of chain end chemistry on the surface relaxation behavior. The apparent shape change in lateral force–scanning rate curves with increasing temperature for the P2VP–$C_2C_8^F$ film seems to be the same as that of the P2VP–H film. However, the relation between the peak position and the temperature differs in the two cases, P2VP–H and P2VP–$C_2C_8^F$. For example, the distinct peak was observed at 343 K for the P2VP–$C_2C_8^F$ film, whereas the P2VP–H film was not the case at the same temperature, as shown in Fig. 3. This means that the thermal molecular motion at the surface of the P2VP–$C_2C_8^F$ film is more active than that of the P2VP–H film at a given temperature. Assuming that a temperature, at which a peak appears on the scanning rate–lateral force curve, almost corresponds to T_g^s, the T_g^s difference in the two samples might be 10 K, as shown in Fig. 3. What is the difference between the P2VP–H and P2VP–$C_2C_8^F$ films is only the chain end structure, as shown in Fig. 1. In the case of P2VP–H, chain ends are composed of a *sec*-butyl group and a repeating unit terminated by proton, whereas end groups of P2VP–$C_2C_8^F$ chain consists of a *sec*-butyl group and a repeating unit terminated by fluoroalkyl group. Since the surface free energy of the fluoroalkyl end group is much lower than that of the repeating unit terminated by proton, it can be reasonably assumed that the surface concentration of the chain end groups for the P2VP–$C_2C_8^F$ film is greater than that of the P2VP–H. This discrepancy results in the difference of surface molecular motion between the P2VP–H and P2VP–$C_2C_8^F$ films.

---

[1] Since polymers used were so fragile due to its smaller M_n, dynamic viscoelastic measurement of the bulk sample was not carried out. Based on Johnson–Kendall–Roberts (JKR) theory, it is conceivable that the scanning rate of 10^3 nm s^{-1} for our current LFM measurements is almost equivalent to the measuring frequency of 70 Hz for dynamic viscoelastic measurements. In the case of such a frequency range, an onset temperature on temperature–E' curve corresponds well to T_g determined by an onset temperature on DSC curve (see Ref. [16]).

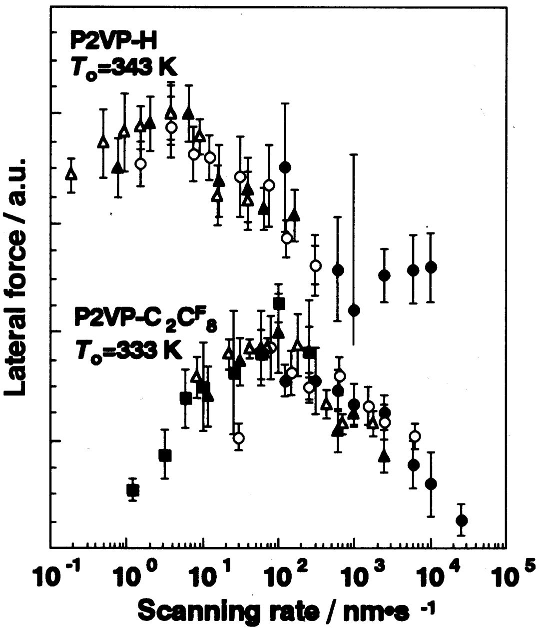

Fig. 4. Master curves of the scanning rate–lateral force relationships drawn from the each curve in Fig. 3. Reference temperatures of 343 and 333 K were used for the P2VP–H and P2VP–$\mathrm{C_2C_8^F}$ films, respectively.

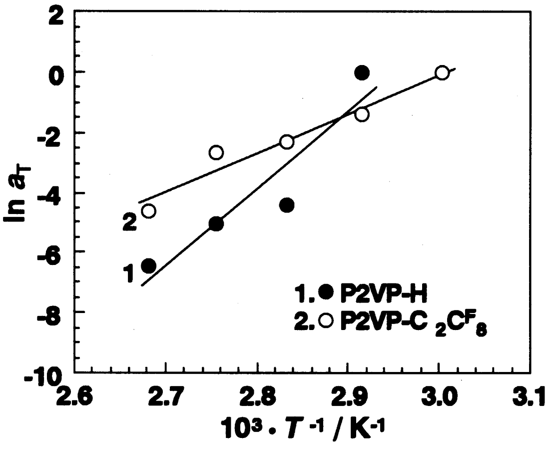

Fig. 5. Semi-logarithmic plots of shift factor, a_T, vs. reciprocal absolute temperature for the P2VP–H and P2VP–$\mathrm{C_2C_8^F}$ films.

Hence, it seems reasonable to conclude that the chain end chemistry is one of the responsible determining factors on surface molecular motion. The shape of each curve in Fig. 3 suggests that the master curves of the lateral force–scanning rate relation would be obtained by the horizontal and vertical shifts.

Fig. 4 shows the master curves for the P2VP–H and P2VP–$\mathrm{C_2C_8^F}$ films drawn by horizontal and vertical shifts of each curve shown in Fig. 3 as the reference temperatures of 343 and 333 K, respectively. Assuming that the shift factor, a_T, has a functional form of Arrhenius type [25,26], the apparent activation energy for the α_a-relaxation process, $\Delta H^{\ddagger}$, is given by

$$\ln a_T = \frac{\Delta H^{\ddagger}}{R}\left(\frac{1}{T} - \frac{1}{T_0}\right) \tag{1}$$

where R is the gas constant, T and T_0 are the measuring and reference temperatures, respectively. Fig. 5 shows the relationships between $\ln a_T$ and the reciprocal absolute temperature for the P2VP–H and P2VP–$\mathrm{C_2C_8^F}$ films, the so-called Arrhenius plots. The activation energies of the surface α_a-relaxation process calculated from each slope shown in Fig. 5 were 220 ± 60 and 110 ± 20 kJ mol^{-1}, respectively, which were much smaller than the reported bulk $\Delta H^{\ddagger}$ of 520 kJ mol^{-1} [27]. The discrepancy of $\Delta H^{\ddagger}$ value between surface and bulk implies that the cooperativity was reduced at the surface due to the existence of the free space on the polymer segments [16]. When the film thickness is comparable to, or less than, the dimension of an unperturbed polymer chain, the polymer chains are supposed to be confined to the narrow space, resulting in the entropy in a chain being affected from the distorted conformation. In addition, the surface/interface area to volume ratio drastically increases for such an ultrathin film. To study how the film thickness influences the surface molecular motion, the lateral force measurement of an ultrathin P2VP–$\mathrm{C_2C_8^F}$ film was carried out. Fig. 6 shows the scanning rate dependence of lateral force as a function of temperature for the P2VP–$\mathrm{C_2C_8^F}$ film with a thickness of 15 nm prepared on the hydrophilic silicon wafer. The radius of gyration, R_g, of an unperturbed P2VP–$\mathrm{C_2C_8^F}$ chain is deduced to be approximately 5.8 nm [28]. Hence, the thickness of 15 nm corresponds to 2.6R_g. The lateral force was not dependent on the scanning rate employed up to 343 K. At 353 K, the lateral force increased with decreasing scanning rate, and then the clear peaks were observed at 363 and 373 K. Here, it should be noted that Fig. 3(b) corresponds to the scanning rate–lateral force relations for the thicker film, 145 nm. In this case, the temperature, at which the peak was observed on the scanning rate–lateral force curve, was 343 K. That is, the surface of the 145 nm thick P2VP–$\mathrm{C_2C_8^F}$ film could reach a glass–rubber transition state at 343 K, which was well below T_g^s of the 15 nm thick P2VP–$\mathrm{C_2C_8^F}$ film. Since P2VP segments might preferably interact with the hydrophilic substrate, the interfacial layer on substrate acts on molecular motion of thin films as an inactive layer in terms of molecular motion. When the film thickness becomes thinner, this interfacial effect becomes remarkable because of the large interfacial area to volume ratio. Therefore, it seems reasonable to conclude that in the case of the 15 nm thick P2VP–$\mathrm{C_2C_8^F}$ film, T_g^s was apparently observed to be higher than T_g^s of the thick film. However, it is interesting to note that even in such an ultrathin film, T_g^s remained lower than T_g^b of 374 K. van Zanten et al. studied the film thickness dependence of T_g of the P2VP–H thin film itself on the hydrophilic silicon wafer, and concluded that T_g of the thin film increased with decreasing film thickness. This is because the effect of the interfacial layer, which is

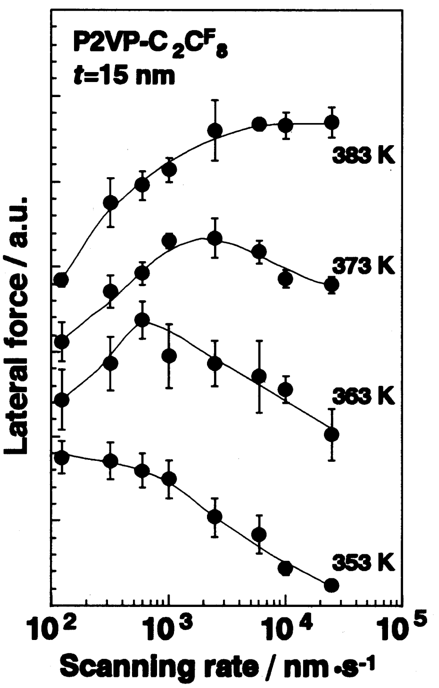

Fig. 6. Scanning rate dependence of lateral force as a function of temperature for the ultrathin P2VP–$C_2C_8^F$ film.

inactive, on the molecular motion of the thin films became dominant with decreasing thickness. Hence, the inclination of the film thickness–T_g relation between surface and thin film was qualitatively the same. However, while T_g^s in the ultrathin film was lower than T_g^b, T_g of ultrathin film itself was higher than T_g^b.

4. Conclusions

Surface molecular motion of P2VP–H and P2VP–$C_2C_8^F$ films was studied by LFM. It revealed that T_g^s was much lower than the corresponding T_g^b due to the surface segregation of chain ends and the reduced cooperativity at the surface. T_g^s increased with decreasing film thickness. However, T_g^s remained lower than T_g^b even for the ultrathin film, with the thickness being comparable to the chain dimension.

Acknowledgements

This was in part supported by a Grant-in-Aid for COE Research (#08CE2005) from the Ministry of Education, Science, Sports, and Culture, Japan.

References

[1] Garbassi F, Morra M, Occhiello E. Polymer surfaces: from physics to technology. Chichester: Wiley, 1994.
[2] Jones RAL, Richards RW. Polymers at surfaces and interfaces. Cambridge: Cambridge University Press, 1999.
[3] Keddie JL, Jones RAL, Cory RA. Europhys Lett 1994;27:59.
[4] Reiter G. Macromolecules 1994;27:3046.
[5] Forrest JA, Dalnoki-Veress K, Dutcher JR. Phys Rev E 1997;56:5705.
[6] Fukao K, Miyamoto Y. Phys Rev E 2000;61:1743.
[7] Schwab AD, Agra DMG, Kim JH, Kumar S, Dhinojwala A. Macromolecules 2000;33:4903.
[8] Fryer DS, Nealey PF, de Pablo JJ. Macromolecules 2000;33:6439.
[9] Keddie JL, Jones RAL, Cory RA. Faraday Discuss 1994;98:219.
[10] Wu WL, van Zanten JH, Orts WJ. Macromolecules 1995;28:771.
[11] van Zanten JH, Wallace WE, Wu WL. Phys Rev E 1996;53:R2053.
[12] Kajiyama T, Tanaka K, Ohki I, Ge SR, Yoon JS, Takahara A. Macromolecules 1994;27:7932.
[13] Tanaka K, Taura A, Ge SR, Takahara A, Kajiyama T. Macromolecules 1996;29:3040.
[14] Kajiyama T, Tanaka K, Takahara A. Macromolecules 1997;30:280.
[15] Satomi N, Takahara A, Kajiyama T. Macromolecules 1999;32:4474.
[16] Tanaka K, Takahara A, Kajiyama T. Macromolecules 2000;33:7588.
[17] Tanaka K, Jiang X, Nakamura K, Takahara A, Kajiyama T, Ishizone T, Hirao A, Nakahama S. Macromolecules 1998;31:5148.
[18] Satomi N, Tanaka K, Takahara A, Kajiyama T. Submitted for publication.
[19] Tanaka K, Satomi N, Yokoe Y, Takahara A, Kajiyama T. In preparation.
[20] Akabori K, Tanaka K, Takahara A, Kajiyama T. In preparation.
[21] Ashley JC. IEEE Trans Nucl Sci 1980;NS-27:1454.
[22] Affrossman S, Hartshorne M, Jerome R, Pethrick RA, Petitjean S, Rei Vilar M. Macromolecules 1993;26:6251.
[23] Minato K, Takemura T. Jpn J Appl Phys 1967;6:719.
[24] Hammerschmidt JA, Gladfelter WL, Haugstad G. Macromolecules 1999;32:3360.
[25] Takayanagi M. Proceedings of the Fourth International Congress on Rheology. London: Butterworth, 1965.
[26] Bueche F. J Appl Phys 1955;26:738.
[27] Takahashi Y, Ochiai N, Matsushita Y, Noda I. Polym J 1996;28:1065.
[28] Bollinne C, Stone VW, Carlier V, Jonas AM. Macromolecules 1999;32:4719.